

Return to Mercury: An Overview of the MESSENGER Spacecraft Thermal Environmental Predictions and Analysis Process

G. Allan Holtzman,¹ Shawn M. Begley,² and Carl J. Ercol³
The Johns Hopkins University Applied Physics Laboratory, Laurel, MD, 20723

At 01:00 UTC on 18 Mar 2011, the MERcury Surface, Space ENvironment, GEOchemistry, and Ranging (MESSENGER) spacecraft became the first to achieve orbit around the planet Mercury. Designed and built by The Johns Hopkins University Applied Physics Laboratory in conjunction with the Carnegie Institution of Washington, MESSENGER was launched on 3 Aug 2004, and after studying the planet Mercury from orbit for more than four years, impacted the planet at 19:25 UTC on 30 Apr 2015. This paper provides an overview of the thermal support activities for the spacecraft and the process used to make temperature predictions for critical spacecraft components. The planned operational profile for the spacecraft position and attitude was run through the thermal analysis process to generate environmental and internal heating profiles for spacecraft components. The environmental heating calculations were performed with a custom algorithm that was run on a graphics processing unit for increased performance and that takes into account the thermal environment of Mercury, including spatial variation of the surface properties. Temperature predictions were generated from physical models of each spacecraft component, and the operational plan was modified if temperature limits were exceeded. Each Mercury year, flight temperatures were compared with the predictions, and adjustments to the process were made as necessary. Special thermal challenges, such as comet observations, instrument calibrations, or potential safe-hold demotions, were analyzed on an individual basis and sometimes involved several iterations of planning. The fidelity of the enhanced thermal analysis process optimized science return while mitigating thermal risks to the spacecraft and its instruments.

Nomenclature

<i>AU</i>	=	Astronomical Unit
<i>CUDA</i>	=	parallel computing platform and programming model created by the Nvidia Corporation
<i>ESC</i>	=	Earth solar constant
<i>FPAA</i>	=	Front phased-array antenna
<i>GPU</i>	=	Graphics processing unit
<i>IR</i>	=	Infrared
<i>MOI</i>	=	Mercury orbit insertion
<i>MTA</i>	=	Mercury true anomaly
<i>OCM</i>	=	Orbit-correction maneuver
<i>OTA</i>	=	Orbit true anomaly
<i>SAX</i>	=	Solar Assembly for X-rays
<i>SciBox</i>	=	An end-to-end automated science planning and commanding system
<i>STK</i>	=	Satellite ToolKit
<i>XRS</i>	=	X-Ray Spectrometer

¹ G. Allan Holtzman, Spacecraft Analysis and Operations Thermal Lead, The Johns Hopkins University Applied Physics Laboratory, 11100 Johns Hopkins Road, Laurel, MD 20723-6099.

² Shawn M. Begley, Instrument Analysis and Operations Thermal Lead, The Johns Hopkins University Applied Physics Laboratory, 11100 Johns Hopkins Road, Laurel, MD 20723-6099.

³ Carl J. Ercol, Spacecraft Design Thermal Lead, The Johns Hopkins University Applied Physics Laboratory, 11100 Johns Hopkins Road, Laurel, MD 20723-6099.

I. Introduction

THE Mercury Surface, Space ENvironment, GEochemistry and Ranging (MESSENGER) mission studied Mercury from orbit for more than four Earth years. This paper provides an overview of the thermal support activities of the MESSENGER spacecraft during the final orbital phase of the mission; the cruise phase, Mercury orbit insertion (MOI), early orbital operations, and the transition to an 8-hour orbit have been covered previously.¹⁻⁵ Spacecraft-related thermal activities included calculations of the thermal heating environment, daily monitoring of the temperatures of spacecraft components and instruments, comparison of flight temperatures with model predictions and historical trends, and interactions with the operations team to manage temperatures of critical spacecraft components.

The thermal environment around Mercury is severe and highly variable. During Mercury's eccentric 88-day orbit, the solar constant varies from 4.7 ESC (planet aphelion is 0.46 AU) to 11.1 ESC (planet perihelion is 0.30 AU), where ESC is the Earth solar constant. Mercury has a high surface emissivity (~0.93, varying slightly with location), rotates very slowly (once every 59 days), and has virtually no atmosphere, causing planet surface temperatures to be very hot on the sunlit side of the planet (up to 451°C at the subsolar point near perihelion) and very cold on the dark side of the planet (-163°C). The temperature distribution on the surface of Mercury at perihelion is shown in Figure 1. The surface temperatures drop off rapidly near the terminator, from 335°C at 60° angular distance from the subsolar point to -163°C on the nightside of the planet.

The orbital geometry for the primary mission (a duration of one Earth year) was chosen via comprehensive thermal analysis⁶ to minimize the effects of the highly varying thermal environment around Mercury. The spacecraft was injected into a dawn-dusk orbit when Mercury was near perihelion, which puts thermally challenging noon-midnight orbits around Mercury true anomaly (MTA) 100° and 280°, the peaks of the two hot seasons that MESSENGER experienced each Mercury year. The

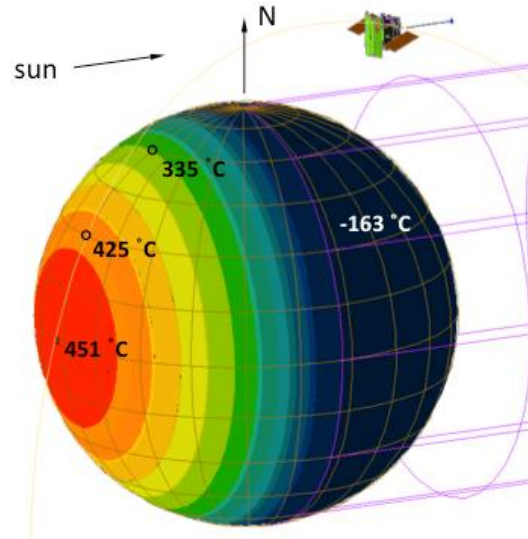


Figure 1. Mercury surface temperature distribution at perihelion.

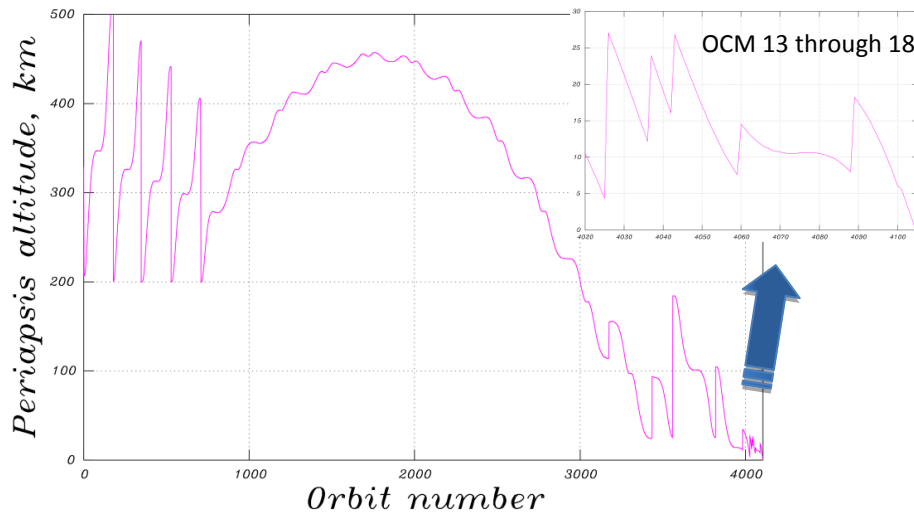


Figure 2. Spacecraft periapsis altitude as a function of orbit number.

orbit plane was relatively inertial with respect to the Sun (unlike a spacecraft in Earth orbit, due in a large part to oblateness of the Earth), so the timing of the hot seasons did not change much for each Mercury year. The initial orbit geometry was 200 × 15,200 km altitude with a period of 12 hours, and orbit-correction maneuvers (OCMs) were periodically performed to readjust the orbit (including a major adjustment to the orbital period to 8 hours). The spacecraft periapsis altitude

versus orbit number is shown in Figure 2. The OCMs during this time are indicated on the chart and generally occurred at Mercury aphelion or perihelion. The last six OCMs were part of the hover campaign, in which gaseous helium was used as a means of propulsion, in addition to the remaining hydrazine.

Although MESSENGER's orbit plane was relatively inertial with respect to the Sun, over the course of the mission the orbital line of apsides rotated around Mercury (because of gravitational forces from Mercury and the

Sun), changing the location of the orbit periapsis relative to the subsolar point (Figure 3). The latitude of periapsis progressed northward from 60°N at MOI to 84°N in 2013 and thereafter southward to 55.7°N at the end of the mission. This drift caused the first hot season (sometimes referred to as low-MTA or outbound season) in each Mercury year to gradually become hotter, because periapsis moved northward and eventually switched to the dayside of the planet during this season, and the second hot season (high-MTA or inbound season) to become less hot. The planetary infrared (IR) heating of the +Y face of the spacecraft (a side mostly insensitive to specific spacecraft maneuvers because the spacecraft is limited to rotations about its Y-axis, with minor exceptions) for Mercury years 3, 10, and 17 is shown in Figure 4. The heating increased with time in the first season, and decreased in the second, as indicated by the arrows on the figure. The orbit average heating values increased slightly with successive Mercury years because of the decrease in orbit period and general lowering of the periapsis altitude.

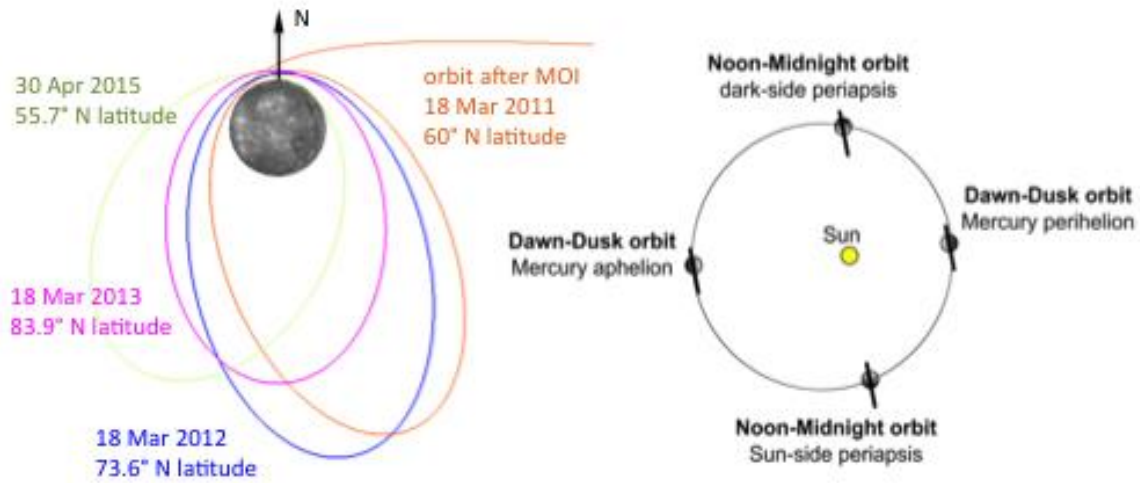


Figure 3. Progression of the latitude of periapsis and inertial orientation of the MESSENGER orbit plane.

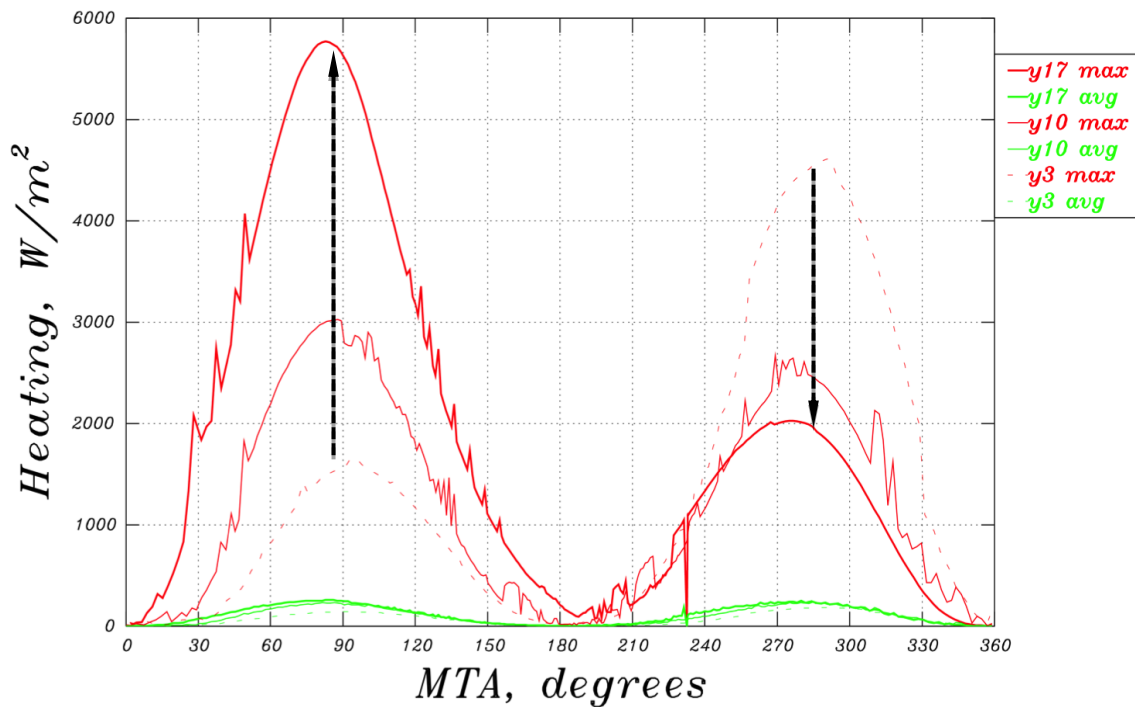


Figure 4. Planetary IR heating of the +Y face of the spacecraft for Mercury years 3, 10, and 17. The heating shown for each orbit includes the peak (in red) and the orbit average (green) values.

The MESSENGER thermal control system was very robust, and the spacecraft performed well over the entire mission, including the change in orbital period from 12 to 8 hours and much lower periapsis altitudes (major changes that were not in the baseline mission design).^{7,8} To survive the intense direct solar heating, the spacecraft had a ceramic-cloth sunshade, as shown in Figure 5, which was oriented toward the Sun, allowing for the use of standard electronics and thermal control materials for most components. Components not protected by the sunshade, such as the solar arrays, were specially designed to survive high temperatures. During noon-midnight-type orbits, the spacecraft passed between Mercury and the Sun, which exposed components behind the sunshade to the substantial, but transient, IR heating from the planet.

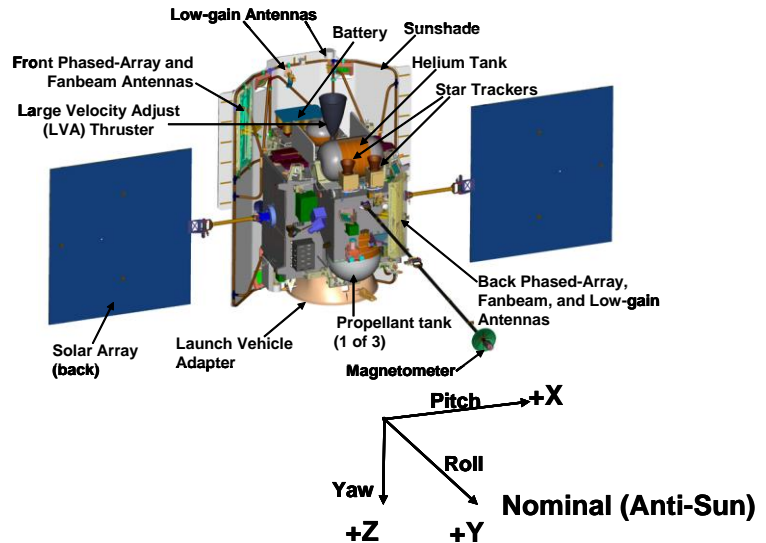


Figure 5. The MESSENGER spacecraft and flight coordinate system.

The heat rates on the $\pm X$ and $\pm Z$ faces of the spacecraft versus orbit true anomaly (OTA) during a portion of a typical orbit in Mercury year 17 near the peak of the first hot season (6 Feb 2015, MTA 88) are shown in Figure 6. The default orientation of the spacecraft was to orient the adapter ring ($+Z$) toward the planet so that remote sensing instruments could collect data from the surface of the planet, which resulted in higher heating on this face. Some components, such as the battery, were positioned on the top deck ($-Z$) such that the spacecraft body blocked the heating from the planet. Other components with dedicated radiators that could not always be directed away from the planet were protected by the use of diode heat pipes (on the $+X$ face), which effectively stopped conducting when the radiator surface became hot and resumed normal operation when the radiator cooled, thereby protecting the electronics from the transient heat pulse. In general, this thermal control approach worked extremely well, and most components on the spacecraft were never a concern. However, there were exceptions that caused deviations from the original operational plan and required attitude adjustments, additional monitoring, and modeling. Three of these components, namely the front phased-array antenna (FPAA), battery, and solar arrays, are highlighted in this paper.

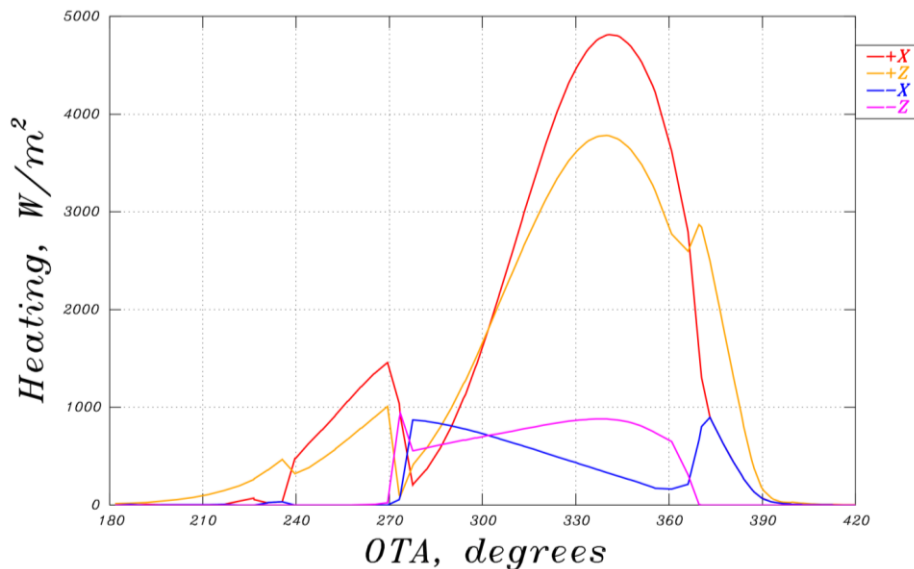


Figure 6. Planetary infrared heating on the faces of the spacecraft, from apoapsis to 60° after periaapsis near MTA 88 in Mercury year 17.

II. Telemetry Processing

MESSENGER thermal telemetry was processed, mainly with MATLAB and shell scripts, on Linux servers several times a day by using cron (a time-based job scheduler). This approach is powerful yet flexible, allowing for such features as extraction of thermal telemetry from any time period over the entire mission within seconds, automated detection and notification of any anomalous thermal telemetry, and autonomous creation of daily temperature and heating plots that showed the current data against the backdrop of previous Mercury years. It is important to note that experience gained from the daily monitoring process led to an increased understanding of the spacecraft and a positive impact on its operations and science return.

Starting at MOI, temperatures from housekeeping telemetry were logged in spreadsheets, organized by orbit and Mercury year. Raw temperatures per orbit were automatically generated by the telemetry processing scripts, which were then placed onto a spreadsheet that was published to a network shared area for accessibility by members of the MESSENGER operations team. The spreadsheet itself contains temperatures summarized per orbit for each Mercury year as well as some tools to plot data versus time, MTA, or OTA.

The summary chart, shown in Figure 7, features both the predicted heating and flight temperatures over a Mercury year, summarized per orbit, and includes a pull-down menu object that allows the user to quickly cycle through all the groups defined within the spreadsheet (a group may contain one or more telemetry identifications, or IDs). Plotted on this chart are the minimum, maximum, and orbit-average heat rates or temperatures for each orbit for several different Mercury years (dynamically selectable in the spreadsheet). The bold lines on the chart represent Mercury year 17, whereas Mercury years 16, 15, and 14 are represented as fainter dashed lines with symbols. Plotting the current data against the context of previous year data allowed for deviations from the normal to be easily discerned.

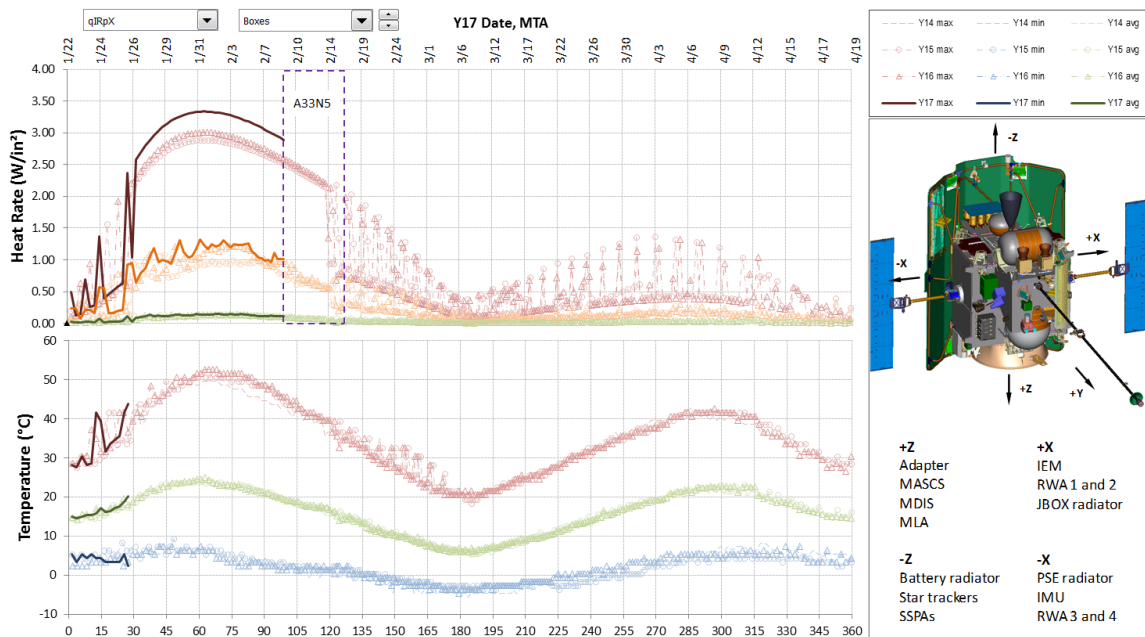


Figure 7. Summary chart of flight temperatures and heating predictions, showing electronic box temperatures for Mercury years 17–14 and environmental heating on the +X side of the spacecraft.

The thermal summary spreadsheet is a very useful data product but took substantial labor to maintain. It is for this reason that an automated process was created, which appended new temperature telemetry to a single file several times per day and also created associated temperature summaries (per orbit) and plots with no user intervention. Command-line plotting tools, coupled with shell scripts and a variety of other software tools (such as sed, grep, and awk), allow for very fast access to any portion of the raw telemetry, which dates back to MOI, within seconds. Time information for each telemetry event included the associated MTA and OTA values, which were automatically added as part of the process. The key to this largely automated process is that it took very little labor to maintain and yet allowed easy access to any level of the data in ways that might not have been previously anticipated (in addition to the standard summary tables and plots). A detailed log file recorded all actions taken by

the autonomous process, in case something unusual occurred. A sample of the type of plot created automatically by the process, just after the peak of Mercury year 17, is shown in Figure 8.

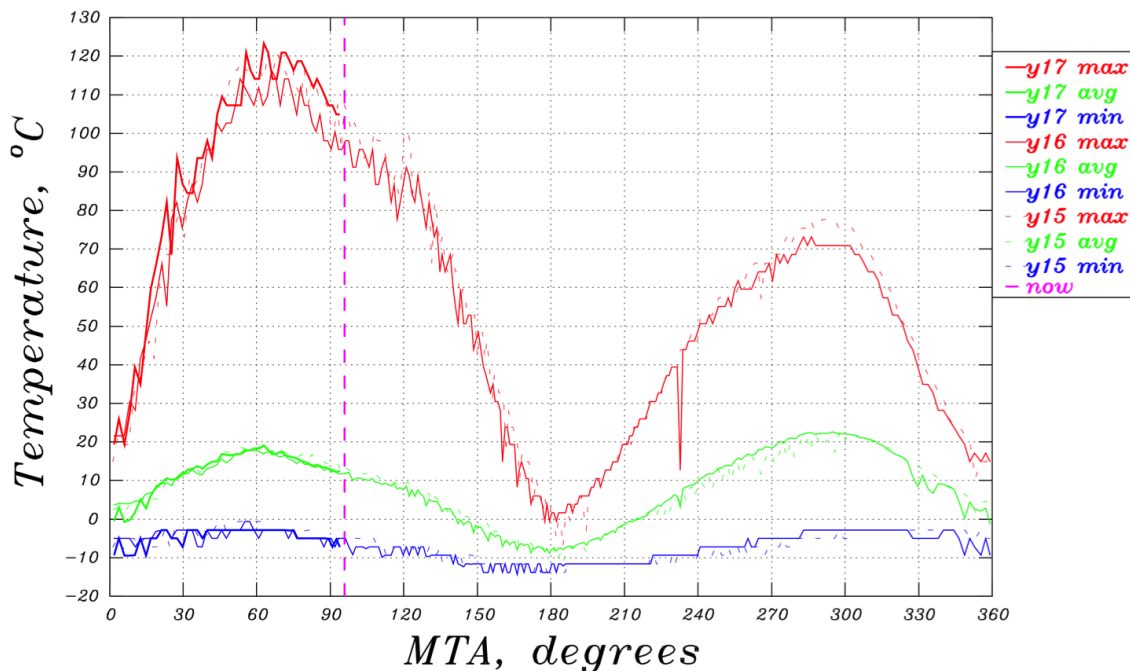


Figure 8. Summary chart from the automated process, showing the orbit peak, average, and minimum temperatures at the adapter ring as a function of MTA for Mercury years 17–15.

III. Heating Algorithm

The thermal environment of Mercury is extreme and variable and was coupled with the operation and changing orbit of the MESSENGER spacecraft, but was proven to be predictable if all of the nuances of the heating environment were considered. Initially, commercial thermal software was used to calculate the environmental heating and make predictions of temperature for critical spacecraft components. However, the need to include more detail from the Mercury heating environment coupled with the higher resolution and longer simulation times quickly became prohibitive to set up and run from a labor standpoint. It is for this reason that thermal heating and temperature predictions for the spacecraft were transitioned to custom algorithms, implemented in the C programming language. All planned maneuvers and science observations were run through this thermal process to ensure the operational health and safety of the spacecraft.

The heating algorithm was designed to be generic, calculating the planetary thermal emission, reflected solar radiation, and direct solar heating on a flat surface in orbit about a planet (or other spherical body). The planet can have varying surface emissivity and reflectivity, and surface temperatures can vary with the direction and magnitude of the solar heating as a function of time (all are relevant for Mercury). The heating is calculated at a given time step by specification of the spacecraft surface orientation and position relative to a fixed planetary coordinate system, along with the solar vector. For the thermal emission or reflected solar calculations, the visible (with respect to the spacecraft) portion of the planet is divided into small areas, and the radiation interchange is calculated on the basis of a flat surface for each differential element. An example of a flat surface oriented toward the planet (divided coarsely for clarity), as well as the planetary elements that contribute to the heating calculation is shown in Figure 9 (in this case, the calculation is reflected solar, so the direction of the Sun is indicated). Planetary surface properties and solar heating are applied on a per-element basis, and the individual element contributions are summed to obtain the total value. The algorithm was implemented initially in MATLAB (for ease of development), translated to Python (for portability and diagnostic capability), and eventually to C (for calculational efficiency). Calculations for flat surfaces in Earth orbit were compared with published data and found to agree to within 0.7% (Figure 10).⁹

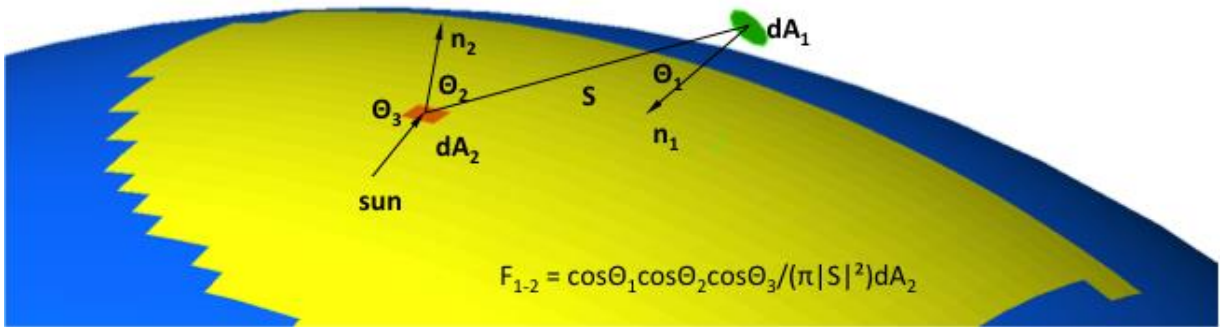


Figure 9. Heating algorithm example showing a reflected solar calculation for a given planetary element to a flat surface in orbit. Planetary elements in view of the surface and the Sun are shown in yellow.

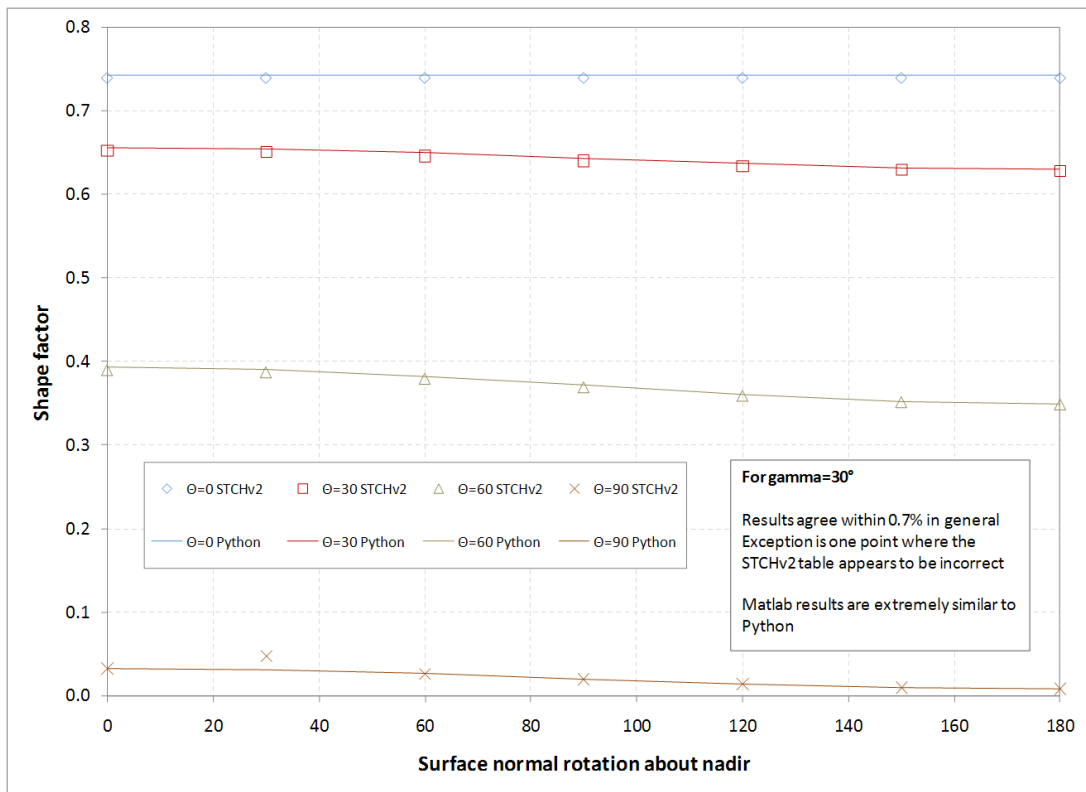


Figure 10. Comparison of heating algorithm results with published data.⁹

For MESSENGER, a wrapper program took a series of orbit positions, attitudes, and solar vectors (provided by SciBox,¹⁰ Satellite ToolKit [STK], or guidance, navigation, and control simulation), passed it to the heating algorithm, and calculated planetary infrared and direct solar heating on a number of spacecraft surfaces (albedo contribution is negligible for Mercury). Because some temperature calculations needed heating specified at fine intervals (down to ≤ 10 s), and simulations sometimes were a Mercury year or longer, the number of time steps for a given scenario might be in the millions. However, heating calculations are independent across time steps, and once implemented on a graphics processing unit (GPU) (with CUDA), the execution time for the heating code was improved >500 times compared with the serial version of the code. This improvement proved to be crucial for MESSENGER, enabling full-Mercury-year and Monte Carlo analyses to be done in minutes, as opposed to weeks or months. It should be noted that the capital investment for this type of capability is hundreds of dollars (for a reasonable GPU, given that a computer is already available to host it). The heating calculation process itself is tailored to the type and format of the input provided, so no additional labor was required for the interface, in contrast to the situation with commercial codes (analyses for which can take considerable time to set up, run, and post-process).

For most spacecraft components, heating on the main faces of the spacecraft was sufficient to predict their thermal response. For others that were nestled somewhat inside the spacecraft structure, such as the battery and FPAA, blockage from the surrounding structure is critical to understanding their thermal response. It is for this reason that the heating algorithm was updated to include this effect. Using ray-tracing techniques, the full spacecraft external geometry was used to determine, for a given surface, directions (in azimuth and elevation) for which incoming radiation is blocked. A look-up table was created for each surface that lists the amount of blockage as a function of azimuth and elevation in spacecraft body coordinates. The heating algorithm references this table to determine how much radiation is blocked for a given planet element, within the discretization loop of the heating algorithm. As an example, the blockage look-up table for the +Z surface of the FPAA is shown graphically in Figure 11. Incident rays are shown for azimuth and elevation angles that are not blocked by other spacecraft surfaces.

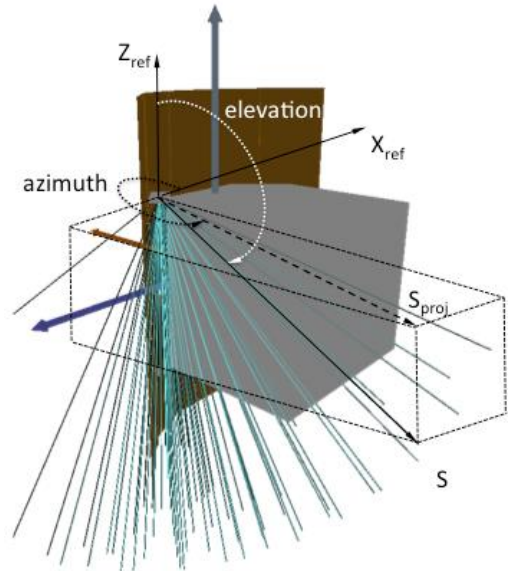


Figure 11. FPAA bottom surface blockage input for the heating algorithm.

IV. Spacecraft Component Models

Special attention was given to critical components on the MESSENGER spacecraft, namely the FPAA, battery, and solar arrays (shown in Figure 5). Thermal models were developed for each of these components and were used to make detailed temperature predictions for all planned operational states, and some that could have happened, such as safe-hold and Earth-acquisition modes. The bulk of the heating data generated for the MESSENGER spacecraft is actually the Earth-acquisition mode for each Mercury year because of the much finer time step and matrix of phase angles to bound all possibilities (the spacecraft did not enter a safe-hold or Earth-acquisition mode at any time during the orbital phase of the mission).

A. FPAA

Analysis of flight data during the first 30 days of the mission (cruise phase) indicated that the signal feeds for the FPAA might exceed their qualification limits during the hottest portions of the Mercury year (Figure 12).¹¹ The feed assembly was soldered with SN63, which has a melting temperature of $\sim 180^{\circ}\text{C}$. Without mitigation, the worst-case scenario might have been loss of high-gain uplink for parts of the mission when the Sun–MESSENGER–Earth angle was $<90^{\circ}$.¹² A plan was put in place to protect the FPAA during the hotter high-MTA season, which rotated the +Z-axis of the spacecraft off-nadir during an OTA range from 320° to 60° . This plan worked well during the primary mission (one Earth year), but as the orbit geometry changed and the spacecraft began to see conditions outside of its original design envelope, the FPAA temperatures reached up to 168°C in flight. The fact that attitudes favorable to the FPAA are unfavorable to the X-Ray Spectrometer (XRS) Solar Assembly for X-rays (SAX) instrument unit complicated the situation considerably.

To solve this problem and bring FPAA temperatures back to just within comfortable levels at the peak of the season, a thermal model was created that takes into account the specific spacecraft attitude profile and trajectory. The portion of the FPAA in question was very lightweight and thus responded very quickly to its environment. It was nestled near the $-Z$ side (top deck) of the spacecraft and against the inside of the sunshade. The FPAA was sensitive to heating on its bottom (+Z) and side ($-X$) surfaces, so the environmental heating was calculated for those surfaces, with blockage of nearby structure. The environmental heating was added to a parasitic heating term from the sunshade (taking into account solar distance and planetary eclipsing) and integrated (with an equivalent space background temperature) to obtain the FPAA temperature predictions.

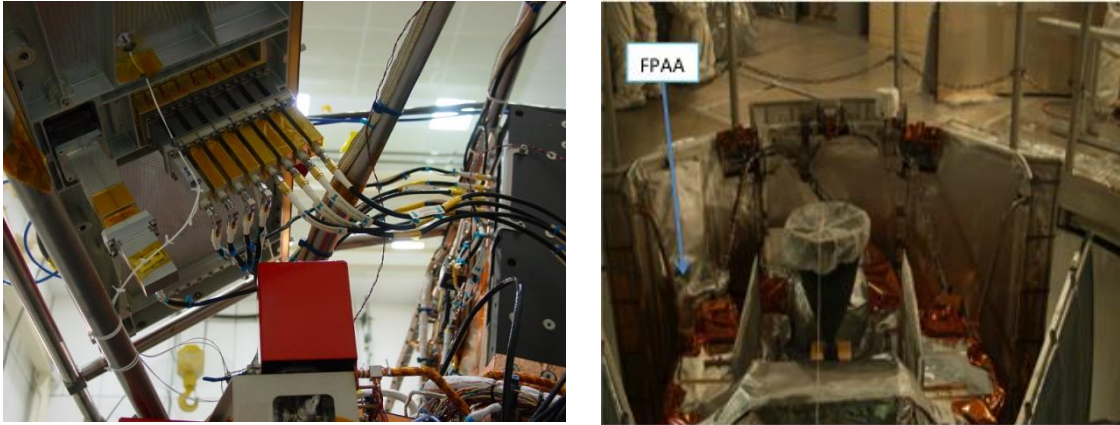


Figure 12. FPAA signal feeds (left) shown before integration with the spacecraft. On the right, the FPAA is shown integrated into the spacecraft with thermal blankets applied.

As shown in Figure 13, the FPAA temperature predictions agree well with the flight data for Mercury year 16, to within $\pm 10^{\circ}\text{C}$ at the peaks of most orbits, with the thermal model slightly overpredicting the peaks where FPAA temperatures are at or near 150°C . A typical orbit is also shown in Figure 13, starting at apoapsis near MTA 90° , 11 Nov 2014. After the FPAA model was developed and tested during Mercury year 16, the generally good agreement between the predictions and the flight data increased confidence in the thermal modeling approach and allowed expanded science operations while still protecting the FPAA during hot portions of the Mercury year.

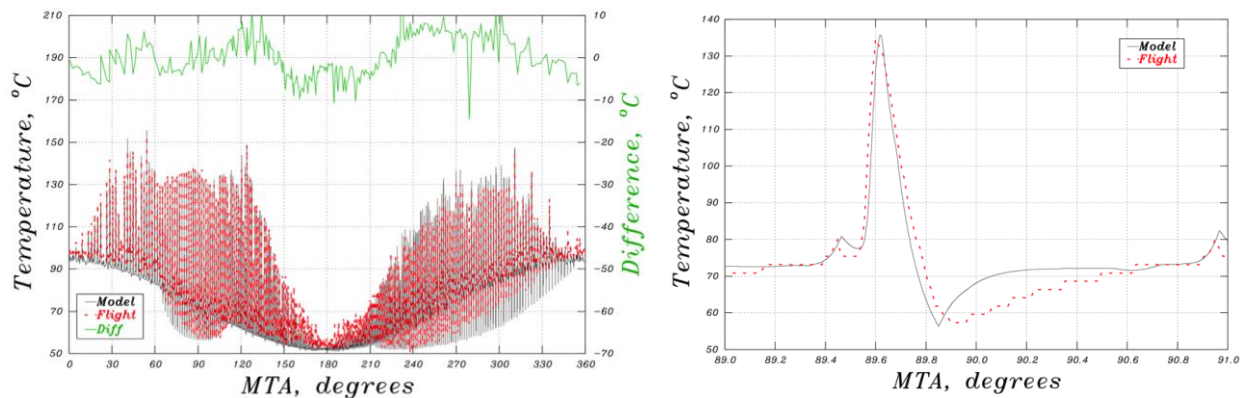


Figure 13. FPAA temperature predictions compared with flight data for Mercury year 16.

B. Battery

Packaged directly behind the sunshade on the $-Z$ deck, the MESSENGER battery consisted of 11 two-cell NiH_2 common pressure vessels housed in a three-piece clamshell-type mechanical design (Figure 14). Although the battery placement provided ideal protection from Mercury's dayside when in orbit, the space-facing radiator used for heat rejection actually received detectable heat input from the back of the sunshade, either from solar heating on the front side or from planetary IR heating on the back. The battery performed very well throughout the MESSENGER mission (temperatures always $<20^\circ\text{C}$), but because it was so vitally important to the mission and had relatively tight temperature constraints, a thermal model that takes into account the thermal environment as well as the electrical dissipation characteristics of the battery was created and correlated to flight data. The thermal model has two nodes, one for the battery cells and another for the radiator. The radiator was near the backside of the sunshade, so blockage from the sunshade was included in the environmental heating on the battery radiator surface. The thermostatic heater was also in the thermal model, with the sensor on the battery cells but heating applied to the radiator, just as in the actual design implementation. The internal dissipation of the battery was very active, and could be exothermic or endothermic at times very close to one another, so the planned (or measured) internal dissipation profile was provided as a function of time by the power team. The environmental heating was applied to the radiator node, on the basis of the spacecraft trajectory and attitude. The battery tended to get warmer for orbits that were favorable to FPAA, but because it was so heavy, it responded to its heating environment slowly and typically took a few orbits for temperatures to ratchet up during the peak of the season.

As shown in Figure 15, the battery temperature predictions agree fairly well with the flight data, generally within 5°C for the peaks of each orbit, over the course of Mercury year 16. With this model, science operations outside of the nominal plan (such as observations of the comets Encke and ISON) were made possible, which would have otherwise been disallowed because of risks to the battery.

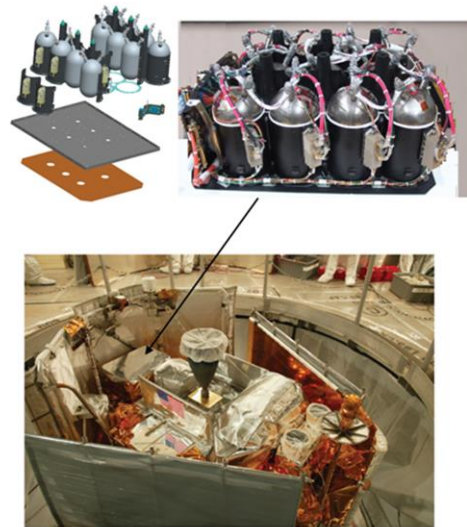


Figure 14. MESSENGER battery design and packaging.

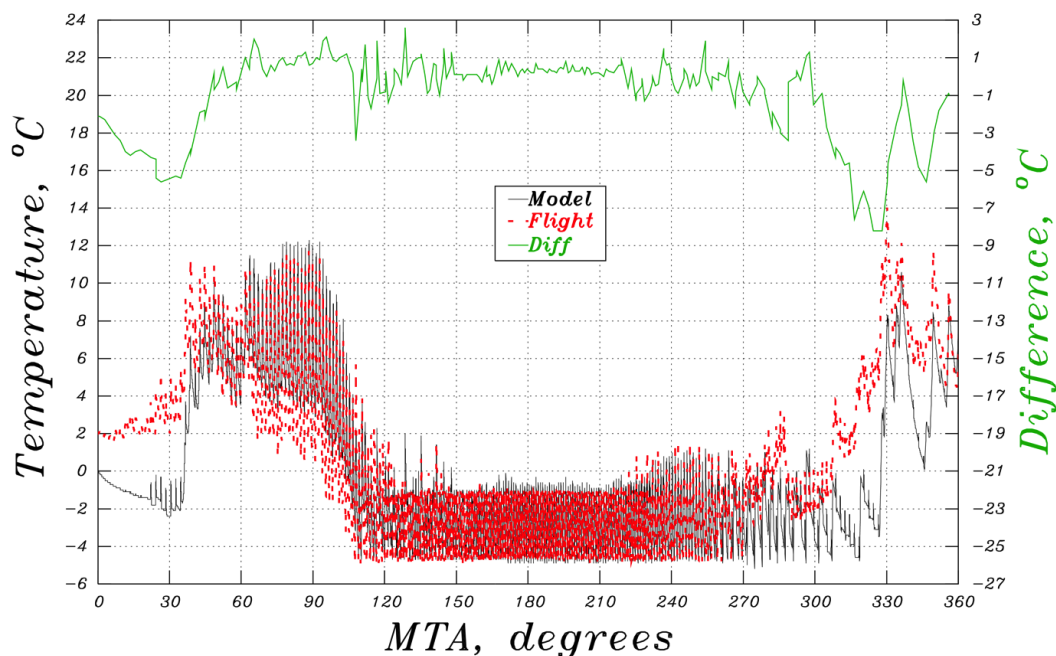


Figure 15. Battery temperature predictions compared with flight data for Mercury year 16.

C. Solar Arrays

The solar arrays each had a 2:1 ratio of optical solar reflectors to triple-junction gallium-arsenide solar cells,^{13,14} as shown in Figure 16, and were managed throughout the Mercury year by pointing them off the Sun by a prescribed amount that increased with higher direct solar heating (because of the eccentric orbit of Mercury). The solar arrays also received planetary IR heating, potentially on both sides, near periapsis, and during the peak of the hotter seasons the solar arrays were commanded to point far off the Sun for a short time to mitigate this transient heat pulse. In later Mercury years, an additional mode was added during which the solar arrays were pointed more off the Sun than normal operations for ~1 hour before orbital peak heating (but not so far as a full offset) in order to pre-cool the arrays. The solar-array commanding was augmented with specific MTA and OTA ranges to off-point the array, and by how much, for every Mercury year (which changed every Mercury year).

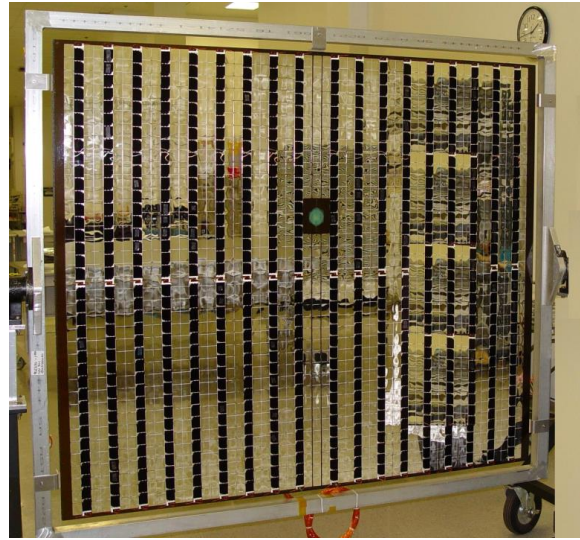


Figure 16. The MESSENGER +X solar array before spacecraft integration.

A solar-array thermal model was created to help plan the operation of the solar-array off-pointing. The model consists of a flat plate, with environmental heating calculated on both sides, rotated about the spacecraft X-axis to the prescribed Sun offset for a given time step. The model can be run in an adaptive mode, where the software attempts to find just-in-time offset values that keep the solar-array temperatures within the specified temperature limit. This procedure helps to define the MTA, OTA, and offset values that should be used for a given thermal season, spacecraft trajectory, and attitude plan. All the points in time for Mercury year 16 where some offset was required to keep the arrays within limit is shown in Figure 17, plotted as OTA versus MTA values. The corresponding Sun offset values as a function of MTA, indicating the severity of the Sun offsets that were required for Mercury year 16, are shown in Figure 18. Once potential limits were defined, the model was run again but in a scripted mode during which the proposed offset profile is implemented and resulting solar-array temperatures are calculated.

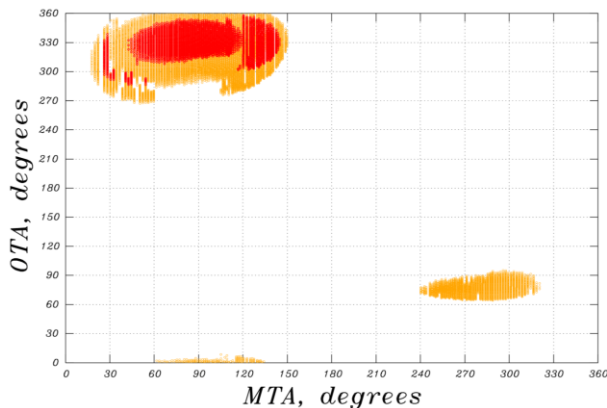


Figure 17. Times versus MTA and OTA when solar arrays are required to point off the Sun more than seasonal amounts during Mercury year 16. Precooling times are indicated in orange, and full-offset times are indicated in red. Note that no full-offsets are required during the high-MTA season.

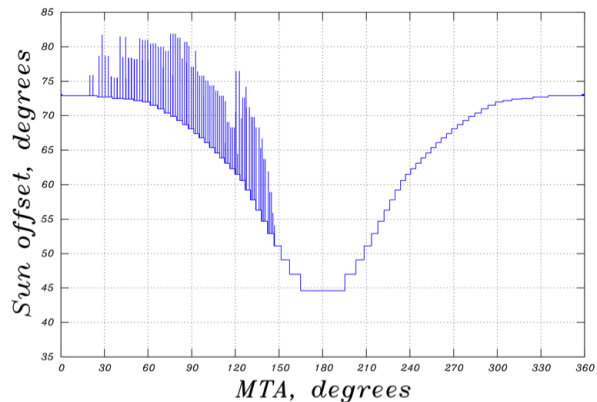


Figure 18. Solar array Sun offset values versus MTA for Mercury year 16. The seasonal offset varies as a function of MTA throughout the Mercury year, and full offsets were needed to mitigate heating from the planet during the first season.

This model allowed for thermal protection of the solar arrays as they experienced the changing solar loads during the Mercury year, as well as the highly transient heat pulses from the planet. As shown in Figure 19, the temperature predictions for Mercury year 16 are within $\pm 20^\circ\text{C}$ of the flight data. The precise timing of the solar-array off-

pointing kept the arrays at or below their prescribed temperature limits while maximizing power generation and overall life.

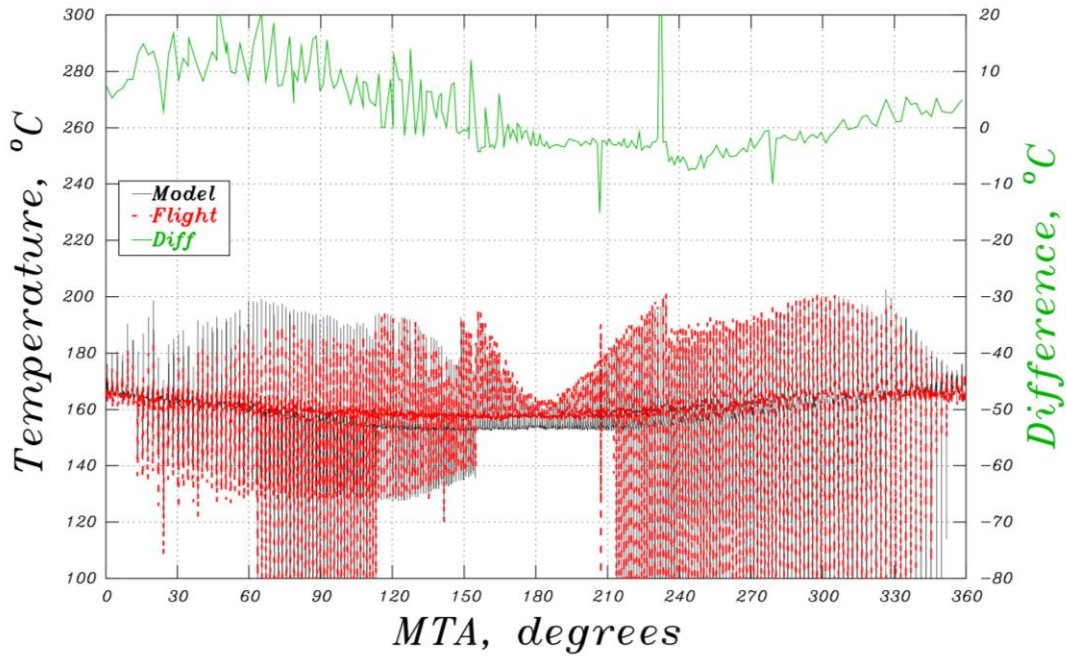


Figure 19. Solar-array temperature predictions compared with flight data for Mercury year 16.

V. End-of-Mission Predictions

FPAA temperatures through the end of mission are shown in Figure 20. FPAA flight temperatures were kept at or below 150°C during Mercury year 17, well below the 180°C limit. For Mercury year 18, the FPAA predictions were allowed to approach 170°C, and flight temperatures were very close to this value (<8°C).

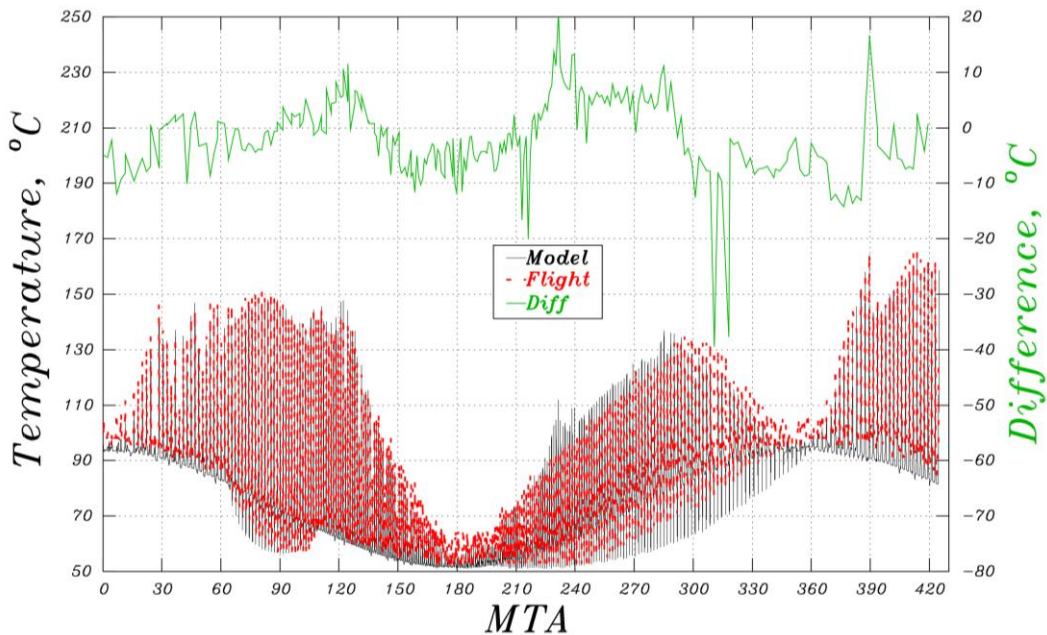


Figure 20. FPAA end-of-mission temperatures, spanning Mercury year 17 and the first part of year 18.

Battery temperatures through the end of mission are shown in Figure 21. Temperature predictions were kept well below 20°C, and, especially in the first season of Mercury year 17, were very close to the flight data (3°C) during that season. The battery temperatures spiked up suddenly at MTA 107 and gradually cooled to match the predictions, which is the same period of time when one of the battery cells exhibited electrical signs of drying out.

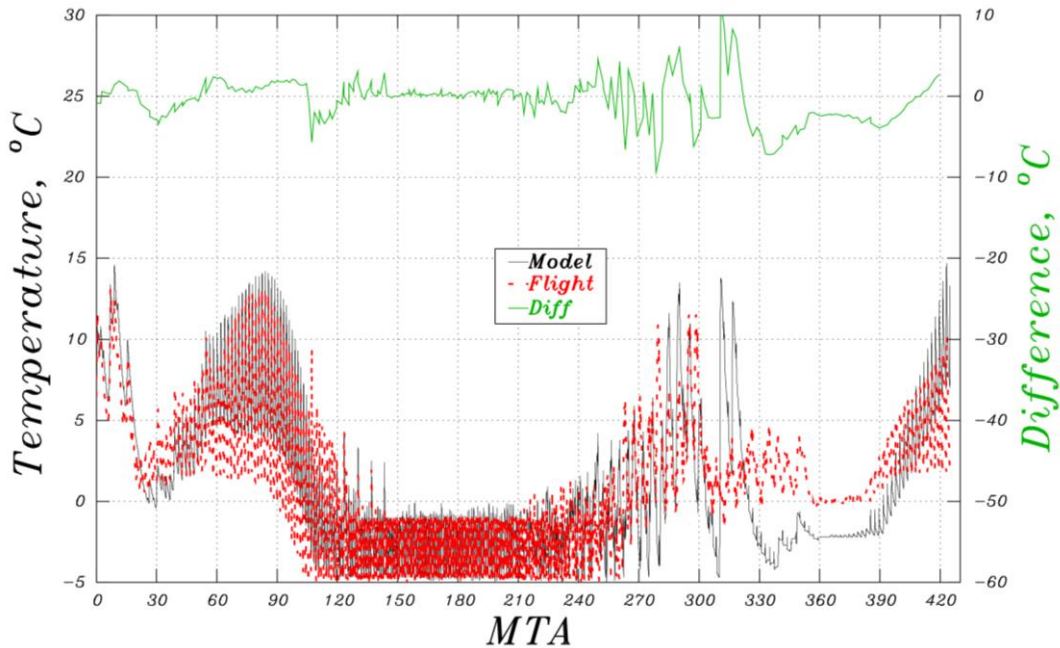


Figure 21. Battery end-of-mission temperatures, spanning Mercury year 17 and the first part of year 18.

Solar-array temperatures through the end of mission are shown in Figure 22. Temperature predictions and flight data generally agreed to within $\pm 20^\circ\text{C}$. The last portion of the mission (Mercury year 18) was thermally challenging, and thus the array temperature limit was raised to 230°C. Array temperatures peaked above 220°C during that time.

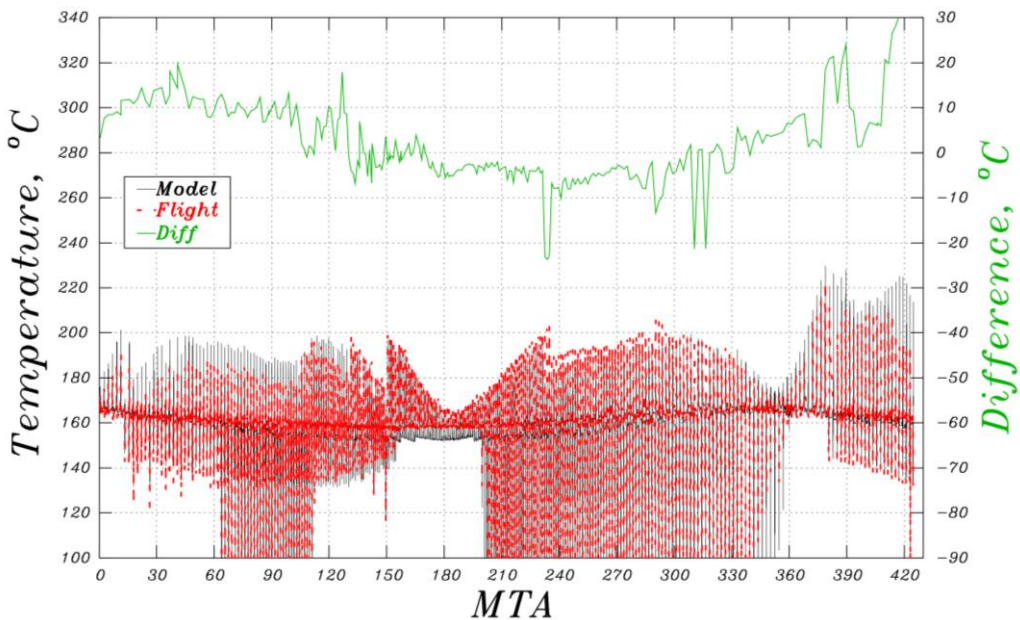


Figure 22. Solar-array end-of-mission temperatures, spanning Mercury year 17 and the first part of 18.

VI. Conclusion

Enhanced thermal support of the MESSENGER spacecraft has allowed the operations team to optimize planned spacecraft maneuvers for maximized science return while mitigating thermal risks to the spacecraft and its instruments. The thermal environment of Mercury is extreme and for the MESSENGER mission was highly coupled with the operation of the spacecraft, but the thermal design of the spacecraft was robust and continued to yield nominal results throughout the mission. In addition, the argument of periapsis for the MESSENGER orbit continued to change, altering the thermal aspects of each Mercury year. This dynamic thermal situation required constant vigilance on the part of the thermal team but also created the opportunity to tie in thermal predictions of the spacecraft with the operational plan to enhance the scientific return from the mission.

Acknowledgments

The MESSENGER mission is supported by the NASA Discovery Program under contracts to the Carnegie Institution of Washington and The Johns Hopkins University Applied Physics Laboratory. The authors acknowledge Sean Solomon, the MESSENGER Principal Investigator at Lamont-Doherty Earth Observatory of Columbia University, and Helene Winters, the MESSENGER spacecraft Project Manager at The Johns Hopkins University Applied Physics Laboratory, for their support in the preparation and presentation of this paper.

References

- ¹Ercol, C. J., Begley, S. M., and Holtzman, G. A., "Return to Mercury: An Overview of the MESSENGER Spacecraft Thermal Control System Design and Up-to-Date On-Orbit Flight Performance," *Thermal and Fluids Analysis Workshop*, paper TFAWS2012-PT-03, 26 pp., Pasadena, CA, 13–17 August 2012.
- ²Ercol, C. J., "The MESSENGER Spacecraft Power System: Thermal Performance through Mercury Flyby 3," *8th Annual International Energy Conversion Engineering Conference*, paper AIAA-2010-6848, 16 pp., Nashville, TN, 25–28 July 2010.
- ³Ercol, C. J., et al., "Power Subsystem Thermal Design and Early Mission Performance," *4th International Energy Conversion Engineering Conference and Exhibit*, paper AIAA-4144, 14 pp., San Diego, CA, 26–29 June 2006.
- ⁴Ercol, C. J., "Return to Mercury: An Overview of the MESSENGER Spacecraft Thermal Control System Design and Up-to-Date Flight Performance," *SAE Int. J. Aerosp.*, Vol. 1, No. 1, April 2009, pp. 405–419.
- ⁵Ercol, C. J., Dakermanji, G., and Laughery, S. C., "The MESSENGER Spacecraft Power System: Thermal Performance through the First Mercury Flyby," *6th Annual International Energy Conversion Engineering Conference*, paper AIAA-2008-5785, 12 pp., Cleveland, OH, 28–30 July 2008.
- ⁶Ercol, C. J., and Santo, A. G. "Determination of Optimum Thermal Phase Angles at Mercury Perihelion for an Orbiting Spacecraft," *29th International Conference on Environmental Systems*, Society of Automotive Engineers, Tech. Paper Ser., paper 1999-01-21123, 10 pp., Denver, CO, 21–25 July 1999.
- ⁷Yen, C. L., "Ballistic Mercury Orbiter Mission via Venus and Mercury Gravity Assist," *J. Astronaut. Sci.*, Vol. 37, 1989, pp. 417–432.
- ⁸Santo, A. G., et al., "The MESSENGER Mission to Mercury: Spacecraft and Mission Design," *Planet. Space Sci.*, Vol. 49, 2001, pp. 1481–1500.
- ⁹Gilmore, D. G., *Spacecraft Thermal Control Handbook Volume 2: Cryogenics*, The Aerospace Corporation Press, El Segundo, CA, 2002.
- ¹⁰Choo, T. H. et al., "SciBox, an End-to-end Automated Science Planning and Commanding System," *Acta Astronaut.*, Vol. 93, 2014, 490–496.
- ¹¹Wallis, R. E., Bruzzi, J. R., and Malouf, P. M., "Testing of the MESSENGER Spacecraft Phased-Array Antenna," *Antenna Measurement Techniques Association 26th Meeting and Symposium*, pp. 331–336, Stone Mountain, GA, October 2004.
- ¹²Flanigan, S. H., O'Shaughnessy, D. J., and Finnegan, E. J., "Guidance and Control Challenges to the MESSENGER Spacecraft in Achieving and Operating from Orbit at Mercury," *35th Guidance and Control Conference, American Astronautical Society*, paper AAS 12-096, 18 pp., Breckenridge, CO, 3–8 February 2012.
- ¹³Wienhold, P. D., and Persons, D. F., "The Development of High-Temperature Composite Solar Array Substrate Panels for the MESSENGER Spacecraft," *SAMPE J.*, Vol. 39, No. 6, 2003, pp. 6–17.
- ¹⁴Ercol, C. J., et al., "Prototype Solar Panel Development and Testing for a Mercury Orbiter Spacecraft," *35th Intersociety Energy Conversion Engineering Conference*, American Institute of Aeronautics and Astronautics, paper AIAA-2000-2881, 11 pp., Las Vegas, NV, 24–28 July 2000.
- ¹⁵Ercol, C. J., "MESSENGER Heritage: High-Temperature Technologies for Spacecraft to the Inner Solar System," *American Institute of Aeronautics and Astronautics Space 2007 Conference*, paper AIAA-2007-6188, 8 pp., Long Beach, CA, 18–20 Sept. 2007.
- ¹⁶Vaughan, R. L., et al., "Return to Mercury: The MESSENGER Spacecraft and Mission," *Institute of Electrical and Electronics Engineers Aerospace Conference*, IEEEAC paper 1562, 15 pp., Big Sky, MT, 4–11 March 2006.